

Study of hybrid passive-active micromixers under an acoustic field

Zahra Ghorbani Kharaji¹, Vali Kalantar^{1,*} and Morteza Bayareh²

¹Department of Mechanical Engineering, Yazd University, Yazd, Iran

²Department of Mechanical Engineering, Shahrekord University, Shahrekord, Iran

*(vkalantar@yazd.ac.ir)

Abstract – This paper presents a numerical investigation of the mixing performance of two hybrid passive-active micromixers subjected to an acoustic field. The study employs the Generalized Lagrangian Mean (GLM) theory and the convection-diffusion equation to analyze concentration profiles within the micromixers, providing a comprehensive assessment of their performance. Perturbation theory is employed to solve the equations of zeroth-, first-, and second-order, resulting in the determination of the final flow velocity from the zeroth- and second-order solutions. Notably, the study incorporates a non-zero background laminar flow to explore the interaction between acoustic waves and a moving laminar flow. The findings reveal that while the presence of sharp-edge structures on the channel walls significantly enhances mixing quality, this improvement is not observed that much when rectangular structures.

Keywords – Perturbation Theory, Microfluidics, Micromixer, Acoustic, Acoustic Streaming

I. INTRODUCTION

Micromixers have gained significant popularity in diverse fields such as medical diagnostics, environmental monitoring, the food and beverage industry, analytical chemistry, biotechnology, and chemical reactions over the past decade. Their ability to facilitate fast reactions between reactants is crucial. However, conventional micromixers encounter challenges related to slow mixing due to low Reynolds number (Re) and reliance on molecular diffusion. To enhance mixing efficiency, two approaches have been employed: passive and active methods.

The passive method involves optimizing the micromixer's geometry, employing features such as spirals, convergence-divergence channels, structured obstacle channels (SAR), and more, to increase the contact surface area between fluids. Previous studies [1-4] have demonstrated substantial improvements in mixing efficiency through passive methods. Conversely, the active

method utilizes external forces, such as acoustics, magnetism, electricity, or heat, to disrupt laminar flow. Earlier research [5-8] has highlighted the effectiveness of the active method in achieving high mixing efficiency in micromixers.

Acoustic flow refers to the stable flow induced by an acoustic field in a fluid, resulting from second-order nonlinear effects arising from the interaction between acoustics and hydrodynamics. Numerous studies have focused on the dynamics of structures under laboratory acoustic fields. Huang et al. [9] conducted one of the pioneering investigations on acoustic flow, experimentally constructing a sharp-edged acoustic micromixer and examining the patterns of acoustic flow around vibrating edges within a microchannel using the Nyberg perturbation technique [10]. Perturbation theory was utilized to numerically investigate the acoustic flow, and the authors presented the effects of various parameters while not considering the initial velocity. Also, Ghorbani et al. [8] performed a

comprehensive numerical study on sharp-edge-based acoustic micromixers, affirming the positive influence of geometrical parameters and acoustic field strength on mixing performance at low Reynolds numbers. They demonstrated that high mixing efficiency (approaching 100%) could be achieved by increasing parameters such as frequency (f), height of sharp edges, and reducing the inlet velocity and angle of sharp edges. Optimal values for the channel width, distance between sharp edges, and the number of sharp edges were also determined.

This study aims to evaluate the performance of three hybrid micromixers that combine active and passive methods. These micromixers feature sharp-edge structures along the channel walls, rectangular structures along the walls, a convergence-divergence section in the middle, and airfoil-shaped obstacles within the convergence-divergence section. An acoustic field is applied throughout the microchannel to enhance mixing. The velocity field is simulated using the Generalized Lagrangian Mean (GLM) approach. Perturbation theory is utilized to solve zeroth-, first-, and second-order equations, enabling the determination of final flow velocity based on zeroth- and second-order solutions. The concentration profile within the entire micromixer is established using convection-diffusion equations. Furthermore, the study investigates the impact of inlet velocity and different geometries on the mixing performance.

II. THEORY

In the context of micromixers, the fundamental equations used to simulate both Newtonian and non-Newtonian fluids are the equations of continuity, momentum, and energy. These equations are mathematically expressed in the form of conservation equations:

$$\frac{\partial \rho}{\partial t} + \nabla \cdot (\rho \mathbf{u}) = 0 \quad (1)$$

$$\frac{\partial \rho \mathbf{u}}{\partial t} = -\nabla \cdot (\rho \mathbf{u} \mathbf{u}) + \rho \mathbf{f} + \nabla \cdot \boldsymbol{\tau} \quad (2)$$

$$\frac{\partial \rho e}{\partial t} = \nabla \cdot (\rho e \mathbf{u} - \boldsymbol{\tau} \mathbf{u} + \mathbf{q}) \quad (3)$$

In the equations, \mathbf{u} represents the velocity vector, ρ denotes density, \mathbf{f} represents the physical force, $\boldsymbol{\tau}$ represents the shear stress tensor, e represents energy, p represents pressure, and \mathbf{q} represents the

heat flux vector. It is important to note that the form of the shear stress tensor varies depending on whether the fluid is Newtonian or non-Newtonian. Additionally, the convection-diffusion transfer equation is expressed as follows:

$$\frac{\partial C}{\partial t} + \nabla \cdot (C \mathbf{u}) = D \nabla^2 C \quad (4)$$

Assessing mixing efficiency is a crucial aspect for all types of micromixers. Various approaches have been developed to evaluate mixing efficiency, and one commonly employed method focuses on the degree of separation. The mixing index (MI), often quantified by the standard deviation of pixel intensity or point concentration, serves as a key parameter for evaluating mixing efficiency. The MI can be mathematically expressed using the following equation:

$$ME = \left(1 - \left(\sqrt{\frac{1}{N} \sum_{i=1}^N \left(\frac{C_i - \bar{C}}{\bar{C}} \right)^2} \right) \right) \times 100 \quad (5)$$

In the equation, C_i represents the pixel density or intensity of the pixel, C denotes the mean concentration or intensity, and N represents the number of sampling points.

To conduct numerical simulations, COMSOL Multiphysics 5.6 software is utilized, employing the finite element method. Table 1 provides the specified parameter values for the water fluid used in the numerical simulation.

Table 1. Parameters utilized in the model (for water, $T=25$ °C).

| Parameter | Value |
|----------------------------------|--|
| Diffusion coefficient, D | $4 \times 10^{-10} \text{ m}^2 \text{ s}^{-1}$ |
| Driving frequency, f | 5.5 kHz |
| Speed of sound (in water), c_0 | 1497 m s^{-1} |
| Displacement amplitude, d_0 | 1 μm |
| Background velocity, v_0 | 500-2000 $\mu\text{m s}^{-1}$ |
| Compressibility, k_0 | $4.48 \times 10^{-10} \text{ Pa}^{-1}$ |
| Shear viscosity, μ | 0.890 mPa s |
| Bulk viscosity, μ_b | 2.47 mPa s |
| Density, ρ_0 | 997 kg m^{-3} |

III. GRID STUDY

In order to address the acoustic physics involving the viscous boundary layer (δ), a more refined computational grid is employed near the walls compared to the bulk geometry. Additionally, the mesh is further refined around sharp edges to investigate the phenomenon of acoustic streaming. To conduct a grid study, the normalized concentration across the channel is assessed at a fixed position (x) with varying grid resolutions. In all meshes, the initial boundary layer thickness is set as $\delta/10$. Fig. 1 illustrates the normalized concentration across the channel at $x = 4200 \mu\text{m}$ for different grid resolutions. Although the normalized concentration remains constant as the degrees of freedom (DOF) increase from 697373 to 950706, the larger DOF is selected for the present simulations to accurately capture the acoustic streaming effects.

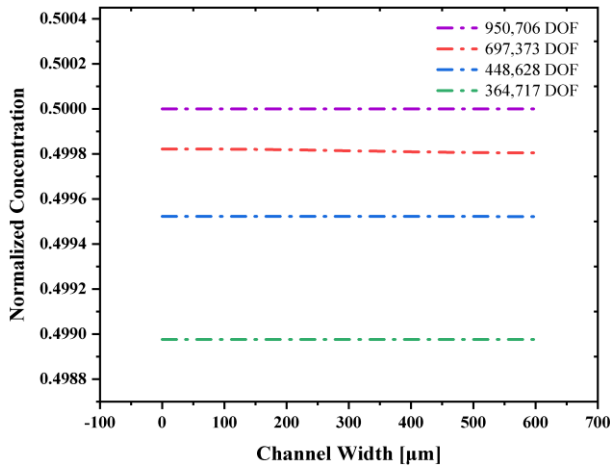


Fig. 1 Normalized concentration across channel width at $x=4200 \mu\text{m}$ for various grid resolutions.

IV. VALIDATION

The present numerical results are verified by comparing them with the experimental data of Nama et al. [11]. The normalized concentration across the channel at $x = 4200 \mu\text{m}$ is calculated for different background velocities (Fig. 2). It can be observed that the present results show good agreement with the experimental data. The maximum error is approximately 5%.

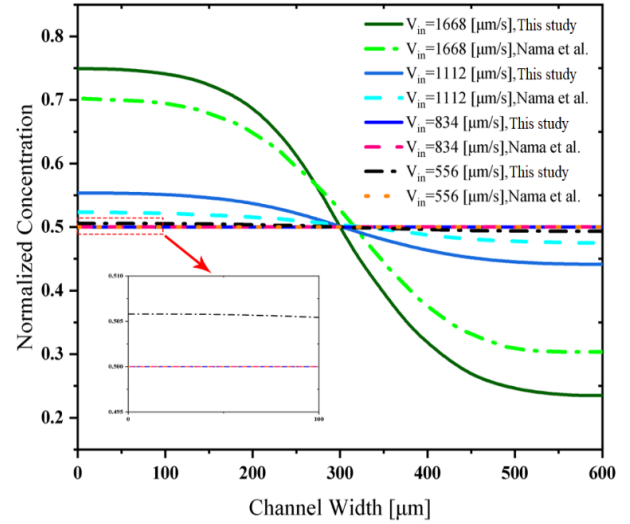


Fig. 2 Normalized concentration across the channel at $x=4200 \mu\text{m}$ for various background velocities.

V. RESULTS AND DISCUSSION

A) An acoustic micromixer with sharp-edge structures

The assessment of the impact of background flow velocity on the mixing efficiency of a micromixer with sharp edges is the focus of this section. This influence is significant since there is no overlap between the background and streaming flows, and changes in the inlet velocity (v_{in}) affect the background and second-order velocities, consequently affecting the mixing process [8, 12, 13]. The investigated background velocities are 500, 900, 1200, and 2000 $\mu\text{m/s}$. Fig. 3a-d presents the concentration profiles for different background velocities in a sharp-edged micromixer when the angle of the sharp edges' tip, the radius of curvature, and the displacement amplitude are $\alpha=15^\circ$, $r_c = 2 \mu\text{m}$ and $d_0=1 \mu\text{m}$, respectively. Additionally, the normalized concentrations across the channel at $x=4200 \mu\text{m}$ for various background velocities are shown in Fig. 4.

The mixing efficiency at the channel output is determined to be 99.98%, 98.29%, 87.975%, and 47.38% for background velocities of 500, 900, 1200, and 2000 $\mu\text{m/s}$, respectively. Notably, complete mixing can be achieved at a low background velocity within a short mixing length (approximately a pair of sharp edges). However, as the background velocity increases and approaches the first- and second-order velocities, the mixing efficiency diminishes. At a high background velocity of 2000 $\mu\text{m/s}$, the mixing performance

remains inadequate even after four pairs of sharp edges, resulting in an extended mixing length. However, when the sharp-edged micromixer is exposed to the acoustic field, the generated acoustic streaming by the sharp edges leads to remarkable mixing at low Reynolds numbers. At high background velocities, the larger and stronger acoustic streaming is suppressed by the background velocity, resulting in a detrimental effect on mixing.

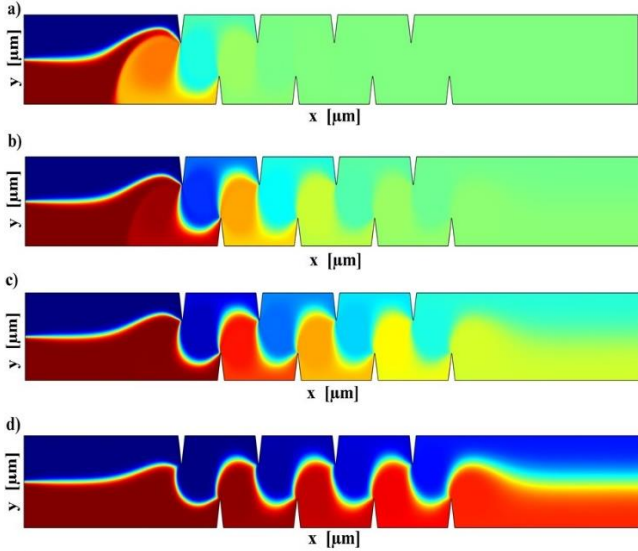


Fig. 3 The concentration profile for various background velocities in a micromixer with $\alpha=15^\circ$, acoustic velocity $v_a = 2\pi f d_0 = 0.062204$ m/s, and $d_0=1$ μm : a $v_{in} = 500$ $\mu\text{m/s}$, b $v_{in} = 900$ $\mu\text{m/s}$, c $v_{in} = 1200$ $\mu\text{m/s}$, and d $v_{in} = 2000$ $\mu\text{m/s}$.

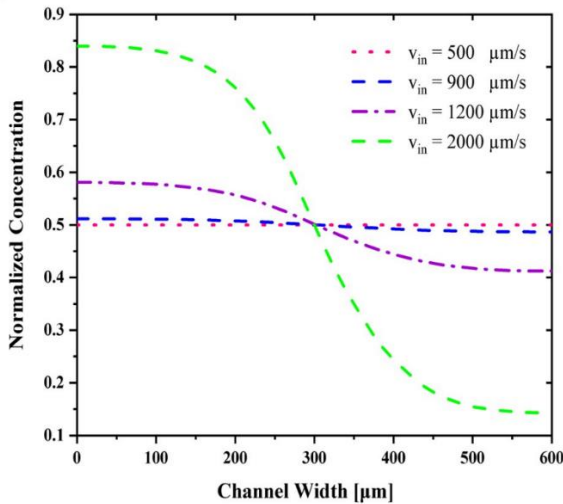


Fig. 4 Normalized concentrations across the channel at $x=4200$ μm for various background velocities.

B) An acoustic micromixer with rectangular structures

An investigation is conducted on an acoustic micromixer featuring rectangular structures with varying heights. The studies in this section consider a background velocity $v_{in}=1200$ $\mu\text{m/s}$, a displacement amplitude value $d_0=1$ μm , and an acoustic velocity $v_a=0.062204$ m/s. The rectangular structures have different height values, and their sharp edges, which have an angle $\alpha = 90^\circ$, are rounded with a radius of curvature $r_c=12$ μm , in accordance with the angles previously used. The height of the studied rectangular structures are 250, 300, and 350 μm . Fig. 5a-c depicts the concentration profiles for the diverse height values of the rectangular structures in this micromixer. Additionally, Fig. 6 presents the normalized concentrations across the channel at $x=4200$ μm for the aforementioned heights of the rectangular structures.

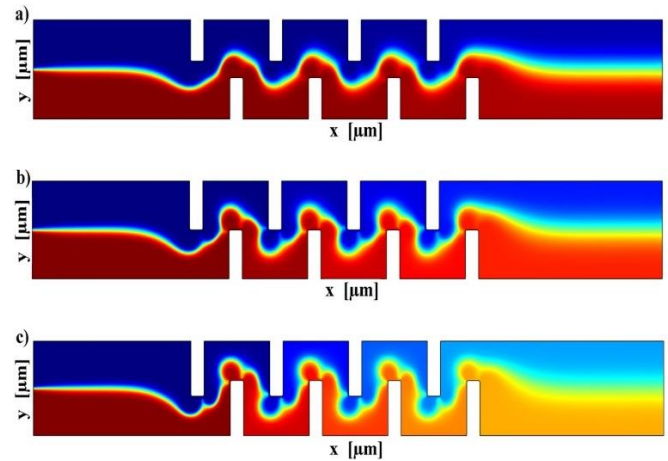


Fig. 5 The concentration profile for various height of rectangular structures in a micromixer with $\alpha=15^\circ$, acoustic velocity $v_a = 2\pi f d_0 = 0.062204$ m/s, $d_0=1$ μm , and $v_{in} = 1200$ $\mu\text{m/s}$: a $h = 250$ μm , b $h = 300$ μm , and c $h = 350$ μm .

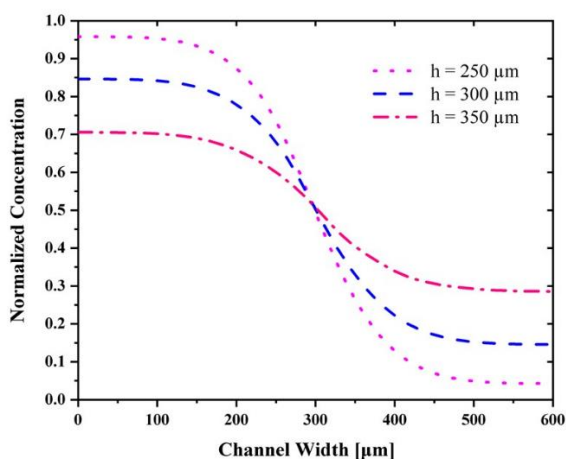


Fig. 6 Normalized concentrations across the channel at $x=4200 \mu\text{m}$ for various height of rectangular structures.

The observations reveal that compared to the sharp-edge structure, weaker acoustic streamings are generated in the case of rectangular structures. This difference heavily relies on the radius of curvature used for rounding the edges, which significantly affects the mixing performance and, consequently, the mixing efficiency in the micromixer with rectangular structures. This outcome is likely due to the formation of smaller and weaker acoustic streamings between the rectangular structures as compared to the sharp-edge structures. It can be attributed to the fact that these structures vibrate less under the acoustic field, affecting the formation of these acoustic streamings. Furthermore, increasing the height of the rectangular structures leads to a smoother normalized concentration distribution across the channel, resulting in improved mixing. The mixing efficiencies at the end of the microchannel, corresponding to the shortest to the tallest height of the rectangular structures, are 27.80%, 45.33%, and 67.93%, respectively.

VI. CONCLUSION

This research undertook a numerical investigation into the mixing capabilities of two acoustic micromixers incorporating sharp-edge structures and rectangular structures. The performance of the micromixers was comprehensively assessed throughout the study. A noteworthy aspect of this research was the incorporation of a background flow, which enhanced the realism of the modeling by encompassing the entire fluidic range. As a result, the need for periodic boundary conditions or extensive layer adaptations was eliminated. The

presence of sharp-edged structures along the channel walls in acoustic micromixers exhibited a substantial enhancement in mixing. However, not that much improvement was observed in micromixers featuring rectangular structures.

REFERENCES

- [1] Jain, S., Unnia, H.N., Numerical modeling and experimental validation of passive microfluidic mixer designs for biological applications, *AIP Adv.* 10 (2020) 105116.
- [2] Bayareh, M., Artificial Diffusion in the Simulation of Micromixers: A Review, *Proc. Inst. Mech. Eng., Part C.* 253 (2020).
- [3] Shiriny, A., Bayareh, M., Inertial focusing of CTCs in a novel spiral microchannel, *Chem. Eng. Sci.* 229 (2021) 116102.
- [4] Bayareh, M., Nazemi Ashani, M., Usefian, A., Active and passive micromixers: A comprehensive review, *Chem. Eng. Process.: Process Intensif.* 147 (2020) 107771.
- [5] Ghorbani Kharaji, Z., Bayareh, M., Kalantar, V., A review on acoustic field-driven micromixers, *Int. J. Chem. React. Eng.* 19 (2021) 553-569.
- [6] Bahrami, D., Ahmadi Nadooshan, A., Bayareh, M., Numerical Study on the Effect of Planar Normal and Halbach Magnet Arrays on Micromixing, *Int. J. Chem. React. Eng.* 18 (2020) 20200080
- [7] Bahrami, D., Ahmadi Nadooshan, A., Bayareh, M., Effect of non-uniform magnetic field on mixing index of a sinusoidal micromixer, *Korean J. Chem. Eng.* 39 (2021) 316–327
- [8] Ghorbani Kharaji, Z., Bayareh, M., Kalantar, V., Acoustic sharp-edge-based micromixer: a numerical study, *Chem. Pap.* 76 (2021) 1721–1738.
- [9] Huang, P.H., Xie, Y., Ahmed, D., Rufo, J., Nama, N., Chen, Y., Chan, C. Y., Huang, T. J., An acoustofluidic micromixer based on oscillating sidewall sharp-edges, *Lab Chip*, 13 (2013) 3847-3852.
- [10] Nyborg, W.L., *Nonlinear Acoustics*, 1998, Hamilton, M. F., and Blackstock, D. T., Academic Press, San Diego, CA.
- [11] Nama N., Huang, P.H., Huang, T.J., Costanzo, F., Investigation of micromixing by acoustically oscillated sharp-edges, *Biomicrofluidics.* 10 (2016) 024124.
- [12] Nam, J., Jang, W.S., Lim, C.S., Micromixing using a conductive liquid-based focused surface acoustic wave (CL-FSAW), *Sens Actuators B Chem.* 258 (2018) 991–997.
- [13] Rasouli, M.R., Tabrizian, M., An ultra-rapid acoustic micromixer for synthesis of organic nanoparticles, *Lab Chip.* 19 (2019) 3316–3325.
- [14] Wang, L., Ma, S., Wang, X., Bi, H., Han, X., Mixing enhancement of a passive microfluidic mixer containing triangle baffles, *Asia-Pac. J. Chem. Eng.* 9 (2014) 877–885.
- [15] Chen, X., Li, T., A novel passive micromixer designed by applying an optimization algorithm to the zigzag microchannel, *Chem. Eng.* 313 (2017) 1406–1414.